Subproject A1.1

Theory of Photonic Crystal Structures and Concepts for Photonic-Crystal based Devices

Principle Investigator: Kurt Busch

CFN-Financed Scientists:

Further Scientists: Thomas Zebrowski

Institut für Theoretische Festkörperphysik
Universität Karlsruhe (TH)

Theory of Photonic Crystals Structures and Concepts for Photonic-Crystal based Devices

Introduction and Summary

Photonic Crystals provide a novel platform for the realization of compact optical elements and novel functionalities. Over the past funding period, the quality of fabrication processes has been significantly improved and novel materials and fabrication routes have been explored. Owing to similar improvements on the theoretical side, the range of applications of Photonic Crystals has been considerably enlarged. This includes, but is certainly not limited to, complex integrated photonic circuits for telecommunication and compact sensors as well as novel light sources such as low-threshold organic lasing structures, efficient LEDs, and directional thermal emitters. The corresponding theoretical challenges are (i) to develop novel simulation methods and tools that are capable of treating ever more complex Photonic Crystal structures, (ii) the predictive and/or interpretative assistance for experimental work in the areas of material science and spectroscopy, and (iii) to develop novel device principles that are exploiting the unique properties of Photonic Crystals.

To address the first of these needs, we have considerably extended the photonic Wannier function approach into a full-fledged circuit theory [1] that allows us to design rather complex Photonic-Crystal based functional elements that include electro-optically tunable materials [2,3]. Further, we have developed a time-domain variant of the Wannier function approach [4]. Our recent review [5] provides an overview of the present state-of-the-art and sketches future research directions, notably in conjunction with Green's functions techniques. In addition, we have equipped our Fourier-Model-Method (FMM) with absorbing boundary conditions based on complex stretched coordinates perfectly-matched layers [6] and the ability to treat internal sources instead of external plane wave excitations. While the former allows us to model non-periodic structures, the latter enables the investigation of active materials in these systems. For metallic systems, however, it turns out that accurate computations require an adaptive spatial resolution for arbitrary geometries of the scatterers. This can be accomplished via numerically determined coordinate transformations [7].

Regarding the second and third challenge, we have employed band structure and FMM computations in order to provide predictive and interpretative assistance for the fabrication and characterization of high-quality three-dimensional Photonic Crystals via holographic lithography [8] and direct-laser-writing approaches [9,10] (collaboration with the group of Martin Wegener, see report on subproject A1.4). Similarly, we have forged a collaboration with the group of Ulf Peschel (University of Erlangen-Nuremberg) in order to investigate polarization-dependent scattering from three-dimensional model Photonic Crystals such as opals [11]. Finally, we would like to mention that a consortium headed by the group of Ralf Wehrspohn (University of Halle) succeeded in demonstrating the feasibility of complex Photonic-Crystal based circuitry by consecutive local infiltration of individual pores [3]. In collaboration with Marian Florescu (Princeton University), we have developed a microscopic theory of thermal emission in bulk Photonic Crystals in thermal equilibrium [12] and have extended this theory to finite-sized systems [13]. The main finding of this work is that the thermal emission enhancement is governed by the area of iso-frequency surfaces – contrary to the commonly held belief that invokes the optical density of states. The corresponding emission characteristics are highly sensitive to the surface termination of the Photonic Crystal. The fact that Kirchhoff's law is a consequence of (and not input to) this theory suggests its extension to the treatment of non-equilibrium situations.

1. Methodic Developments for the Quantitative Analysis of Photonics Crystal Structures

Significant advances in the fabrication of Photonic Crystal structures allow for the realization of ever more complex Photonic-Crystal based circuitry and/or high quality three-dimensional Photonic Crystals. Our strategy to meet the correspondingly increasing demands in quantitative simulations has been to further develop our photonic Wannier function approach [14] as well as the Fourier Modal Method (FMM; sometimes also referred to as the Rigorous Coupled Wave Analysis).

1.1. The Photonic Wannier Function Approach

Since we feel that the modeling, design and optimization of large-scale Photonic Crystal structures will quickly place severe demands on general-purpose Maxwell-solvers, we have significantly extended the photonic Wannier function approach. This extension consists of improvements in the generation of Wannier functions, their application to the construction of Wannier functions for Photonic-Crystal membranes and three-dimensional Photonic Crystals, and the realization of Wannier-function based circuit theory for complex functional elements in two- and three-dimensional Photonic Crystals and Photonic-Crystal membranes as well as an efficient time-domain version of the Wannier function approach.

1.1.1 Wannier Function Generation

More precisely, we have perfected the construction of maximally localized photonic Wannier function based on an adaptation of the method proposed by Souza, Marzari, and Vanderbilt for electronic systems [15,16]. In electronic systems, there exists a Fermi level so that for most applications only the Wannier functions associated to the electronic bands in the immediate vicinity of the Fermi level have to be taken into account. In photonic systems, however, a Fermi level does not exist, so that generally more Wannier functions have to be generated that allow for a correct representation of the details of the electromagnetic field distributions. In fact, this task may quickly become rather challenging, since higher-frequency bands tend to be strongly entangled without band gaps separating them into groups. As a result, a significant symmetry mixing between bands occurs which impedes the construction of well-localized Wannier functions. Thus, a thorough group theoretic preprocessing of the band structure that effectively groups the bands prior to minimization becomes a must. This dramatically reduces the number of unknowns. At the same time, advanced techniques that efficiently minimize the spread of the Wannier functions can dramatically decrease computation times. While the above issues appear to be a rather technical, they are at the heart of the entire approach since only a sufficient number of Wannier functions that fully conform to the symmetry of the underlying lattice provide quantitative results for functional elements (see the description of the circuit theory below). The resulting enhancement in efficiency can easily decrease the computational effort by about three orders of magnitude relative to a naïve approach. At the same time, this leads to higher-quality Wannier functions.

As an illustration, we provide in Figs. 1 and 2, respectively, examples of photonic Wannier functions for two-dimensional macroporous-silicon Photonic Crystals and three-dimensional silicon-woodpile Photonic Crystals.
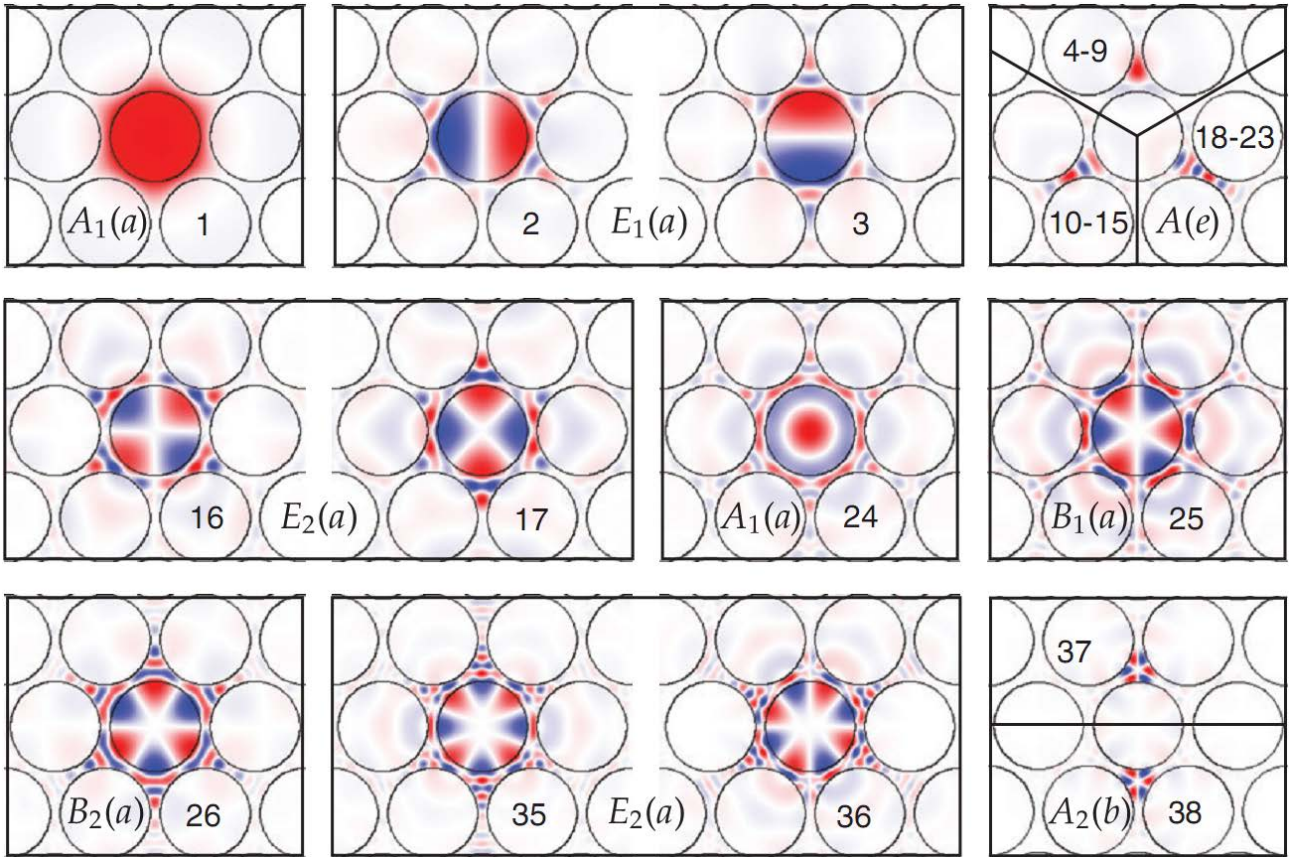
Fig.1: Maximally localized photonic Wannier functions related to the 38 lowest bands for H-polarized light in a two-dimensional Photonic Crystal consisting of a hexagonal array of air pores with radius $r = 0.45a$ (a: lattice constant) in a silicon matrix. The value of the out-of-plane component of the magnetic field is shown. Each Wannier function is labeled by its band index n and, in addition, the group-theoretical labeling is provided. The Wannier functions associated with bands 4-9, 10-15, and 18-23 can, respectively, be obtained from the three representative functions shown in the center of the figure through successive 60° rotations.
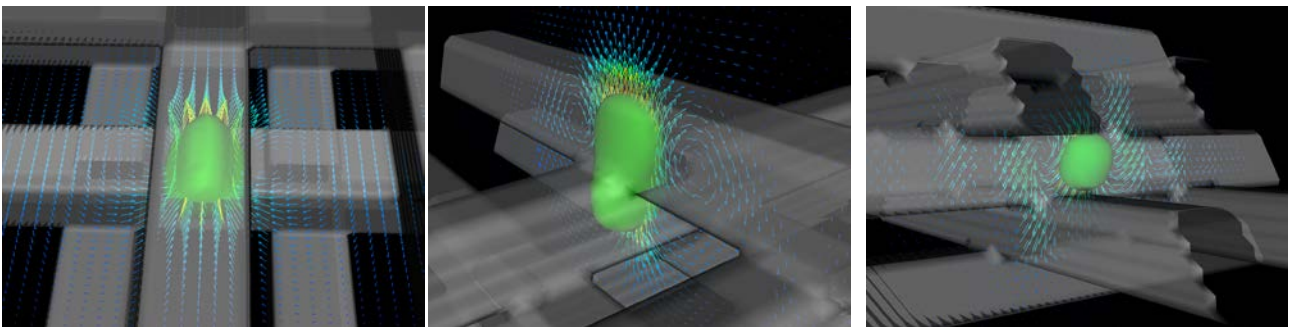

Fig.2: Maximally localized photonic Wannier functions for a three-dimensional woodpile Photonic Crystal. The left and middle panel represents, respectively, the Wannier functions for bands three and four, whereas the right panel depicts the Wannier function for band ten. Owing to the three-fold rotational symmetry of this rhombohedral structure, the Wannier function for band ten occurs three times and the missing functions may be obtained via 120° rotations of the band ten Wannier function around this symmetry axis.

1.1.2 Wannier-function based Photonic Crystal Circuit Theory

The Wannier function approach is ideally suited for the analysis of basic functional elements since the Wannier function basis results from a unitary transformation of the underlying Photonic Crystal's Bloch function basis. As a result, the Wannier basis contains the entire information of corresponding band structure and – as compared to all-purpose Maxwell-solvers – only a few Wannier functions are required to obtain quantitative results. This facilitates the optimization of designs for such functional elements [1,3,5]. Despite the advances in computational efficiencies offered by this approach, large-scale Photonic-Crystal based circuits still require formidable computational resources. Therefore, we have developed a circuit theory [1] that allows us to treat large-scale circuits. Basic functional elements are represented through their complex scattering amplitudes that connect the modes in the various waveguide ports that terminate the device. Then, a complex circuit that consists of an assembly of several basic functional elements can be represented by a scattering matrix. In turn, this scattering-matrix can be obtained from the basic elements' scattering matrices by "integrating out" the internally connected ports. This is analogous to the Landauer-Büttiker approach for mesoscopic electronic systems or the linear system approach in microwave circuit theory. In fact, many complex functional elements contain several copies of just a few basic functional elements, albeit with different orientations. This implies that we can reuse the scattering matrices of given functional elements if we respect the corresponding symmetries [1]. We illustrate this approach in Fig. 3 for a Mach-Zehnder interferometer.

At any rate, the central prerequisite is the usage of Wannier functions whose symmetries conform to the symmetries of the underlying Photonic Crystal. Already minor deviations from the correct symmetry lead to slightly asymmetric scattering matrices for the basic functional elements which – owing to the coherent nature of the coupling between elements – quickly amplify for more complex circuits and unphysical behavior develops.
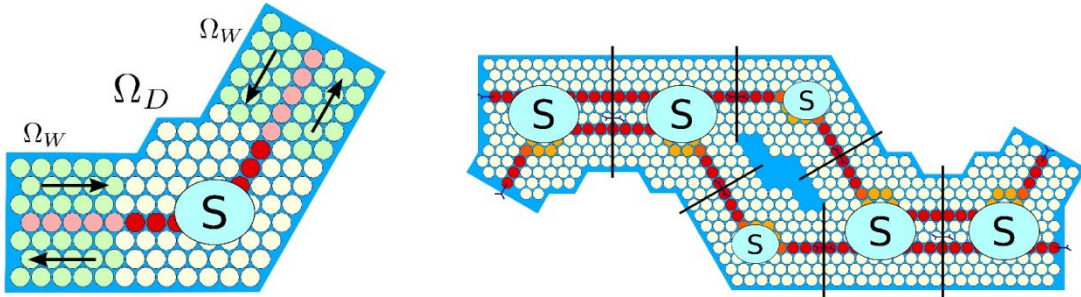

Fig.3: Schematic illustration of the analysis of functional elements within a Wannier-function based Photonic Crystal circuit theory. Left panel: A single functional element (here: a waveguide bend) is connected to several (here: two) waveguide ports. In the wave guiding regions Ω_w (shaded regions), the electromagnetic field is described by incoming and outgoing guided modes that are determined within a separate Wannier-function computation for the infinite waveguides. In the central region, Ω_D, the electromagnetic field is directly expanded into Wannier functions. This allows us to compute the complex reflection and transmission amplitudes between the modes in the wave guiding ports. In essence, this reduces the functional element to a complex scattering matrix. Right panel: Complex functional element can often be decomposed into basic functional elements so that their scattering matrix can be built up from the scattering matrices of the constituents. Typically, the basic functional elements appear multiple times albeit with different orientations. This can be accounted for via appropriate symmetry considerations. We display a Mach-Zehnder interferometer design which is composed of only two distinct basic functional elements, a waveguide bend (lower case *S*) and a coupler end point (upper case *S*), which we have optimized separately.

1.2. The Fourier Modal Method

At the start of the funding period, we had available an implementation of the basic Fourier Modal Method (FMM; sometimes also referred to as the Rigorous Coupled Wave Analysis (RCWA)) for two- and three-dimensional layered grating structures [17]. We have applied this method to a number of interesting problems [8,9,10,11] (see also section 2.2.). However, as explained in section 2.2. a significant number of problems of current interest are outside the reach of basic FMM. Therefore, we have taken up recent developments pioneered in the group of Philipe Lalanne (Institute d'Optique, Palaiseau) and have implemented absorbing boundary conditions based on a complex stretched-coordinate formulation [6]. This allows us to surround parts of the unit cell or the entire unit cell used in the FMM calculations with perfectly-matched-layer-like boundary conditions. As seen from an FMM point-of-view that deals with an infinite array of periodic unit cells this procedure effectively decouples the unit cells partly or completely from each other. If we now send in an excitation onto this structure, we obtain – from a beam-propagation point of view – a fully vectorial, bi-directional eigenmode-based beam propagation algorithm. Furthermore, many physical systems require that the emission characteristics of a dipole source embedded in them are determined. Consequently, we have further extended the FMM such that we can choose between the traditional incoming plane wave excitation and the internal excitation via a point dipole. Since this, too, is well documented in the literature [18], we refrain from describing the details.

However, with all these extensions, efficient computations for arrays that contain significant amounts of metal are still rather challenging. Here, the equidistant grid implied by the Fast-Fourier-Transform of the material distribution within a single unit cell leads to stair-casing of rounded geometries. In turn, this introduces spurious resonances (actually many small lightning rods that constructively or destructively interfere) that are extremely difficult to deal with and simple grid-refinements (corresponding to more plane waves within FMM) become rather ineffective. One way out has been described by Thomas Weiss and coworkers [19]. For specific geometries, they constructed analytical coordinate transformation that concentrate coordinate lines near the material interfaces. Upon working on equidistant grids in this transformed space, one, therefore, realizes an adaptive spatial resolution (ASR). In turn, ASR greatly accelerates convergence or equivalently, for a given desired accuracy, considerable reduces the usage of computational resources. However, these analytical meshes have two drawbacks. First, the associated coordinate transformation is not everywhere differentiable and thus may lead to spurious resonances (albeit very many fewer than in the standard FMM approach). Second, it is unclear whether any geometry may be meshed in this fashion and even if this were the case, it remains unclear (or at least a horrendously difficult task) how to create meshes for more complex geometries. Depending on one's viewpoint, one may regard these issues as some sort of nuisance or as some serious problem for the method. At any rate, it is highly desirable to obtain an automated way to numerically determine differentiable meshes for arbitrary geometries. We have accomplished this task by developing an appropriate functional that allows to adapt coordinates to a given geometry at hand such that the resulting mesh is still differentiable [7].

For simple geometries, we obtain comparable results as Thomas Weiss and coworkers [19] and the resulting convergence acceleration (or, equivalently, accuracy and efficiency improvements) persist also for more complex geometries where it is not obvious how to determine an analytical transformation in the first place. We illustrate this behavior in Fig. 4. Here, one should bear in mind that the storage and CPU-time requirements for such computations scale, respectively, with the square and the cube of the number of plane waves.
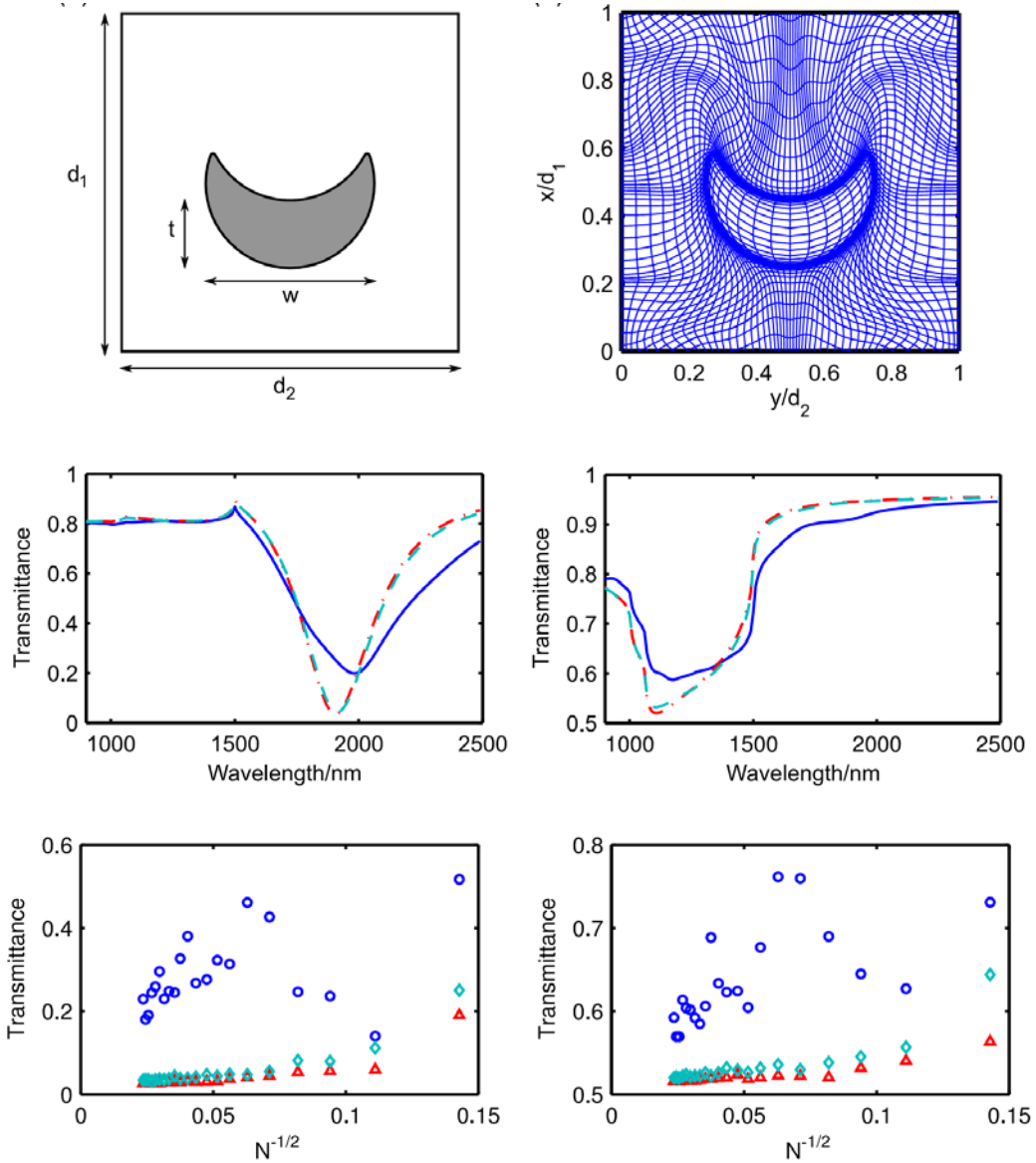
Fig.4: <u>Upper row:</u> Schematic top view a single unit cell of a square array of gold crescent-shape nano-antennas (left panel) and corresponding numerically generated ASR.

<u>Middle row:</u> Transmittance spectra into the zeroth diffraction order that have been computed within standard FMM (blue solid line) using 1257 plane waves, numerical ASR with tangential term (red dash-dotted line) using 317 plane wave and numerical ASR without tangential term (cyan dashed line) again using 317 plane waves. The computations have used y-polarized incoming radiation (curves with pronounced resonances near λ ≈ 1900 nm) as well as x-polarized radiation (curves with pronounced resonances near λ ≈ 1100 nm).

<u>Lower row:</u> Convergence characteristics of the transmittance into the zeroth transmittance. N denotes the number of plane wave coefficients used. The computations have been carried out using standard FMM (blue open circles), numerical ASR with tangential energy term (red open triangles), and numerical ASR without tangential term (cyan open diamond) within FMM. The left panel depicts the case of y-polarized excitation at λ = 1900 nm with ε = −175.08+21.43i (gold at λ = 1900 nm) and the right panel depicts the case of x-polarized excitation at λ = 1100 nm with ε = −53.21+4.20i (gold at λ = 1100 nm).

2. Predictive and Interpretative Assistance for Experimental Work

The experimental realization of large-scale and high-quality Photonic-Crystal structures represents a challenge to state-of-the-art micro-fabrication technologies. Therefore, it is of paramount importance to characterize the optical quality of fabricated samples. For thin films, this can readily be accomplished via electron microscopy. However, samples with an appreciable thickness have to be characterized optically, i.e., their transmission properties have to be determined experimentally (preferably with absolute units) and have to be compared with corresponding simulations. Only this allows the assessment of the fabricated structures' quality as well as the identification of problems in the fabrication process.

The group of Martin Wegener has perfected the so-called direct laser writing technique, where a focused laser beam writes tiny structures ("voxels") into a film of photo-resist via two-photon absorption processes. Moving the focus in a prescribed fashion through the resist thus allows them to write essentially arbitrary structures. Clearly, the details depend on the photo-resist, the precise shape of the focused laser beam inside the sample and the ability to move the focus within the sample (in practice, one rather moves the photo-resist relative to a fixed laser spot). However, the resulting polymer templates exhibit an insufficient refractive-index contrast that prevents the formation of complete, i.e., three-dimensional photonic band gaps. Consequently, this mandates that the polymer templates be replicated into a high-index material such as silicon. Obviously, the many processing steps involved in this provide ample opportunities for fabricating structures with compromised functionality. Just how much can be determined by comparing experimental data with accurate computations on ideal structures. Further, computations on less ideal structures allow one to identify (and potentially to remedy) problems in the fabrication process [8].

With this combined experiment-theory approach, the groups of Martin Wegener and Kurt Busch have been able to systematically optimize the fabrication process so that eventually complete photonic band gaps at 1.55 μm could be reached [9] and basic functional elements such as straight waveguides could be reliably fabricated and characterized [10].

Polarization-resolved reflection and transmission spectra represent a particularly useful tool for the investigation of the quality of three-dimensional Photonic Crystals. Based on this observation, we have, in a collaboration with the group of Ulf Peschel (University of Erlangen-Nuremberg), demonstrated that the growth-mode of opal-like structures via Langmuir-Blodgett (forced-assembly) and self-organized approaches exhibit rather different optical properties that render the (in certain communities rather well-established) concept of the critical angle of diffraction meaningless [11].

3. Novel Concepts for Photonic-Crystal based Functional Elements

Besides being of importance for interpreting experimental data, the methodic developments described in section 1 allow us to explore novel systems as well as to develop novel operation principles for functional elements, including novel functionalities.

3.1 Nonlinear Wave Propagation in Photonic-Crystal Waveguide-Resonator Systems

One of the simplest classes of bistable optical devices that can find applications in photonic integrated circuits are two-port devices where the transmission properties to the output waveguide depend on the intensity of light sent to the input waveguide. In systems where the two waveguides

are directly coupled via an optical resonator, a system with resonant transmission in a narrow frequency range is realized. Alternatively, systems with side-coupled cavities exhibit similar behavior that is, however, based on resonant reflection. Indeed, both systems may exhibit optical bistability when the resonator is made of a Kerr nonlinear material. The resonant two-port devices of the first type can be realized in one-dimensional systems and, consequently, they have been studied in great details in the context of different applications. In contrast, resonant devices of the second type can only be realized in higher-dimensional structures and their functionalities are not yet completely understood. For instance, until recently it has been believed that the basic properties of devices based on resonators side-coupled to ordinary ridge waveguides are qualitatively identical to those of resonators side-coupled to Photonic-Crystal waveguides and that both can be correctly described via standard coupled-mode theory for continuous systems. In Fig. 5, we show the results of our analyses [20] that illustrate the much richer behavior of waveguide-resonator systems in Photonic Crystals as compared to systems based on ordinary waveguide-resonators. The crucial point is that the discrete nature of the Photonic Crystal waveguide allows the engineering of physically inequivalent coupling-scenarios between the side-coupled cavity and the cavities that make up the Photonic Crystal waveguide. This is schematically depicted in the left panel of Fig. 5. There, the case (b) shows a strong coupling of the side-coupled cavity A_α to the nearest cavities A_0 and a much weaker coupling to the next-nearest cavities A_{-1} and A_1. This suggests that this case if conceptually very close to the case of ordinary coupled-mode theory depicted in case (a), since one there, too, assumes a point-like coupling between continuous waveguide and the resonator. Consequently, we call this case "on-site coupled" and we have shown that this case can be mapped onto standard coupled-mode theory [20]. However, the situation is entirely different in case (c), where by construction, the side-coupled cavity A_α experiences identical coupling to the nearest cavities A_{-1} and A_1 (we call this the "inter-site coupled" case). In turn, this leads to novel interference mechanisms that strongly modify already the linear transmission, notably in the slow light regime [20]. In the middle and right panel of Fig. 5, we display the corresponding results of realization of cases (b) and (c) in two-dimensional Photonic Crystals.

The anomalously high transmission in the slow-light regime for the inter-site coupled case allows for a significant enhancement of the resonator quality factor and, accordingly, a substantial reduction of the bistability threshold. As a consequence, we refer to this type of nonlinearity enhancement as a geometric enhancement. The possibility for such enhancements is a direct and unique consequence of the discreteness of the Photonic Crystal waveguide and is in a sharp contrast to similar resonant systems based on ridge waveguides. In Fig. 6, we display the corresponding bistability results for the on-site and inter-site coupled systems described in Fig. 5.

The potential of this type of the nonlinearity enhancement may be regarded as an additional argument to support the application of Photonic-Crystal devices in integrated photonic circuits. The actual experimental realization of such devices would require carefully optimized designs and this represents a serious challenge for computations. First, the system is numerically large, i.e., comprises many Photonic-Crystal unit cells. Second, the presence of nonlinear materials precludes an analysis in the frequency-domain but time-domain simulation in the slow-light regime together with the expected large field-enhancements at the cavity require very long simulation times.

These considerations have been a major modification for developing a Wannier-function based time-domain simulation tool [4] which still requires further developments before it can be applied to the above-described systems.
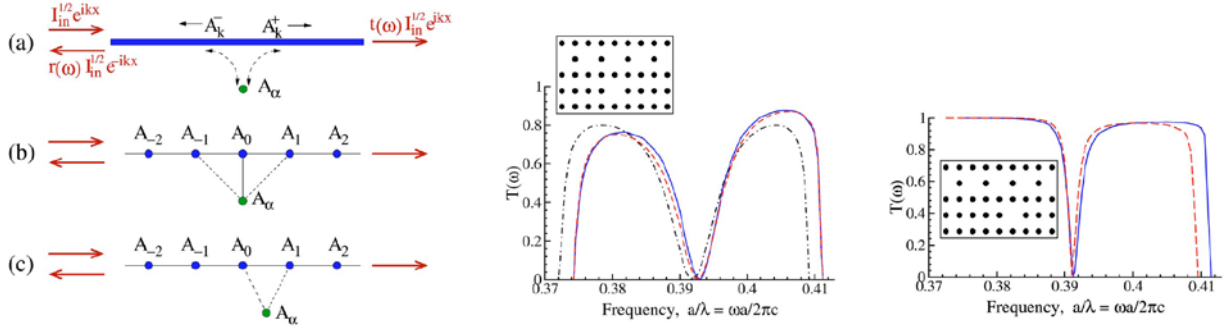
Fig.5: Left panel: Three types of geometries of a straight Photonic-Crystal waveguide that is side-coupled to a nonlinear optical resonator A_α. Standard coupled-mode theory is based on the geometry (a) which ignores effects that are induced by the discreteness of the Photonic-Crystal system. For instance, light transmission and bistability behavior are qualitatively different for on-site (geometry (b)) and inter-site (geometry (c)) locations of the resonator along the Photonic-Crystal waveguide. Middle and right panel: Linear transmission through with silicon-rod based Photonic-Crystal waveguide system with different types of side-coupled resonators. The perfect Photonic Crystal waveguide exhibits a slow-light regime for dimensionless frequencies between 0.37 and 0.38. In this regime the results for on-site and inter-site coupled resonators are significantly different so that vastly different bistability behavior can already be anticipated. We compare exact numerical results (solid line) with different approximations (dashed and dashed-dotted lines). For details we refer to Ref. [20].
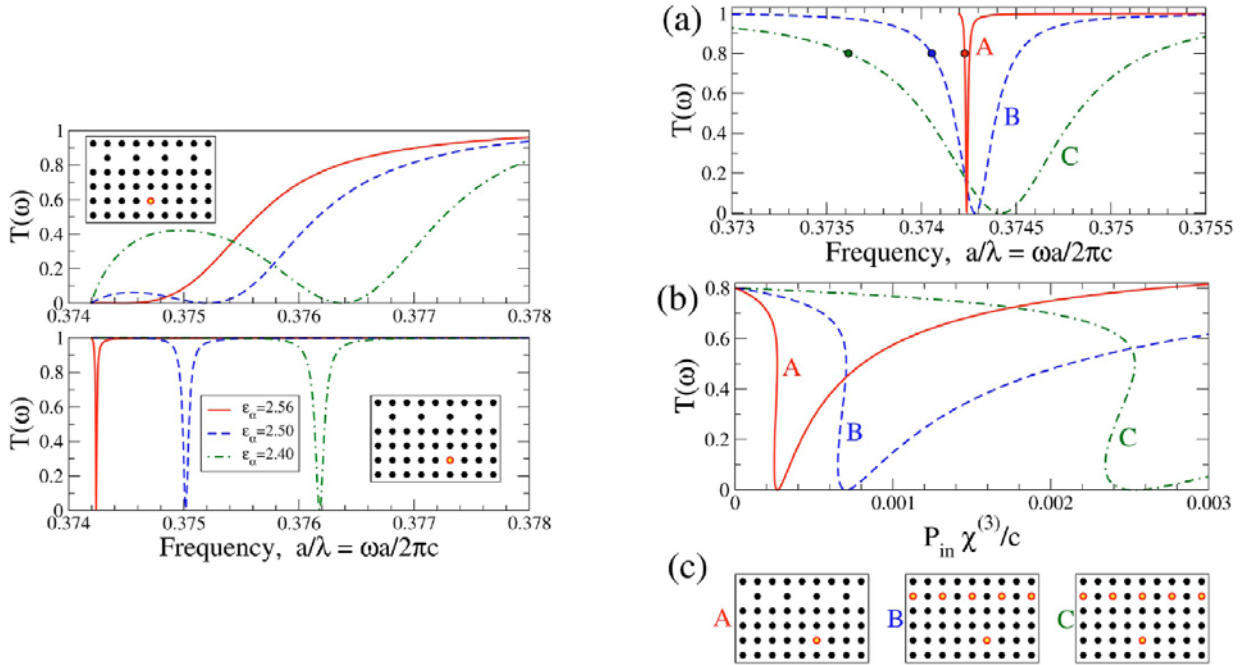

Fig.6: Left panel: Linear transmission spectrum for a silicon-rod based Photonic-Crystal waveguide that is side-coupled to a single on-site (a) or inter-site (b) polymer-rod resonator (red open circle) with different values of the dielectric constant. Right panel: Linear transmission spectra, (a), and nonlinear bistable transmission, (b), for three distinct silicon-rod based Photonic-Crystal waveguides with Kerr-nonlinear polymer rods (red open circles). The corresponding geometries are depicted in subfigure (c). Example A represents a close-to-optimal structure with an inter-site

coupled resonator whose resonance frequency lies close to the edge of the passing band, i.e., in the slow-light regime. Examples B and C represent, respectively, sub-optimal designs with inter- or on-site coupled resonators whose resonance frequencies lies near the center of the passing band, i.e., outside the slow-light regime. The full circles in (a) indicate the frequencies where the transmission reaches 80% and that are used for achieving high-contrast bistable behavior. Due to its poor linear transmission characteristics, on-site coupled resonators cannot be utilized in the slow light regime.

3.2 Thermal Radiation in Photonic Crystals

From the standard definition of a blackbody system, it follows that for any frequency and direction, the flux of the thermal radiation emitted by any material object cannot exceed that emitted by a blackbody at the same temperature and placed in the same environment. This definition is independent of the nature of both the blackbody object and its electromagnetic environment, and does not impose any limit on the amount of thermal radiation emitted by the blackbody. In general, the photonic reservoir of the surrounding medium may support photon modes whose distribution depends on frequency and propagation direction, and the same blackbody object that in free space emits an isotropic thermal flux may inside a Photonic Crystal emit a thermal flux that is enhanced or reduced relative to Planck's law.

We have analyzed the origin of thermal radiation enhancement and suppression inside infinite Photonic Crystals [12]. Standard theoretical and experimental studies of the thermal radiation emitted by Photonic Crystals consult the spectral dependence of the photonic density-of-states (DOS) [21,22] to interpret their findings. While in simple cases this may lead to correct qualitative predictions, we have shown that the central quantity that determines the thermal radiation characteristics such as intensity and emissive power is the area of the iso-frequency surfaces and not the DOS. The basic idea here is that radiation transport via the modes of Photonic Crystals is described through the energy current density, which, in turn, is given by a sum of the product of group velocity and energy density over all modes. In essence, only the energy density is given by the DOS. More precisely, our careful analysis of the radiative properties of a photon gas in an infinite photonic crystal in thermal equilibrium [12] shows profound departures from the conventional model of a blackbody in free space. For frequencies near van Hove singularities, the spectral energy density as well as the thermal radiation flux may exceed the corresponding quantities for a blackbody in free space. There are two mechanisms contributing to this enhancement. First, similar to a homogeneous dielectric medium, the photonic crystal constitutes an optically denser effective medium than free space. The second mechanism originates from the strong light scattering that leads to a spectral redistribution of the photonic modes. We have shown that the thermal flux must be compounded with an additional factor of the group velocity such that the standard interpretation of thermal radiation characteristics in photonic crystals—and other strongly scattering systems—via the DOS becomes questionable. Instead, the area of the iso-frequency surface relative to that of free space becomes the quantity that determines the enhancement of blackbody radiation in Photonic Crystal. This is illustrated in Fig. 7, where we display the frequency dependence of energy density and spectral hemispherical power length for a two-dimensional model system and compare the results to the free space values. Moreover, the thermal radiation in Photonic Crystals shows focusing effects along specific crystalline directions, which may directly impact future applications.
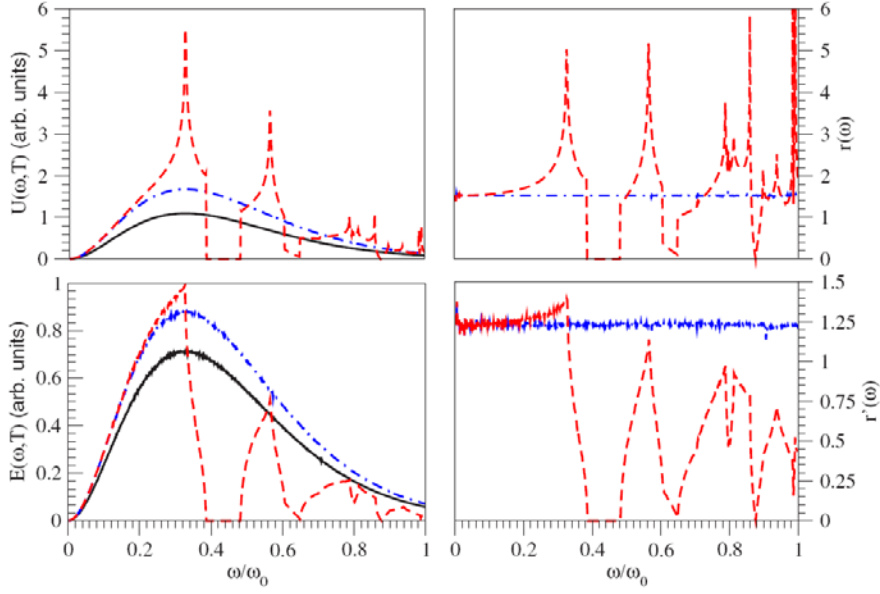
Fig.7: Frequency dependence of the spectral energy density (upper left panel) and the spectral hemispherical power (lower left panel) for the free space (continuous line), a homogeneous dielectric with dielectric constant equal to 1.52 (dashed-dotted line), and a model Photonic Crystal with a long wavelength effective dielectric constant equal to 1.52 (dashed line). The temperature is chosen such that the conventional blackbody exhibits a maximum at the frequency of the first van-Hove singularity of the model system's density of states at $\omega = 0.327\omega_0$. The frequencies are measure in units of $\omega_0 = 2\pi c/a$, where a denotes the lattice constant of the Photonic Crystal (see Ref. [12] for further details). The upper and lower right panels show the enhancement of the respective quantities relative to their free space value.
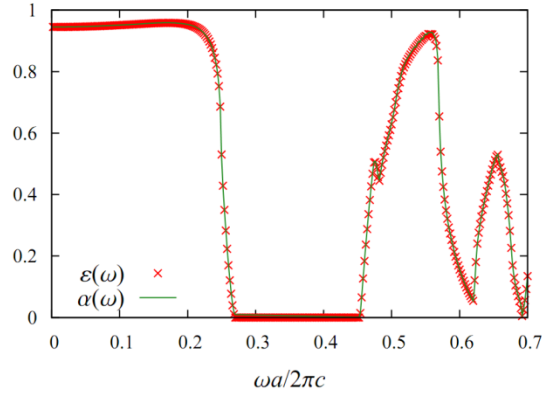

Fig.8: Hemispherical spectral emissivity computed from our theory (solid line) and absorptivity computed via FMM (symbols) of a two-dimensional model Photonic Crystal emitting into an air half-space. Obviously, Kirchhoff's law is obeyed.

To this end, we have extended our analysis to the case of finite Photonic Crystals as well. In this case, it is necessary to include the transmission and reflection of radiation at the interface between a Photonic Crystal and its surroundings. Simple thermodynamic considerations show that these scattering processes <u>must</u> reduce whatever enhanced thermal flux is forming within the Photonic Crystal in a manner such that the radiation emitted by the Photonic Crystal into, say, an adjacent half space of air is consistent with Kirchhoff's law. In other words, Kirchhoff's law which is not

directly contained in our theory becomes a consequence for the case of thermal equilibrium. Thus, our theory represents a potential starting point for the development of a more sophisticated theory that would be able to consider non-equilibrium scenarios.

Besides this more fundamental aspect our theory also allows for the computation of other quantities such as directional emissivities and, for instance, facilitates the investigation of just how the surface termination of Photonic Crystals may be exploited to construct thermal emitters with desired (or prescribed) properties. In Fig. 9, we provide an illustrative example.
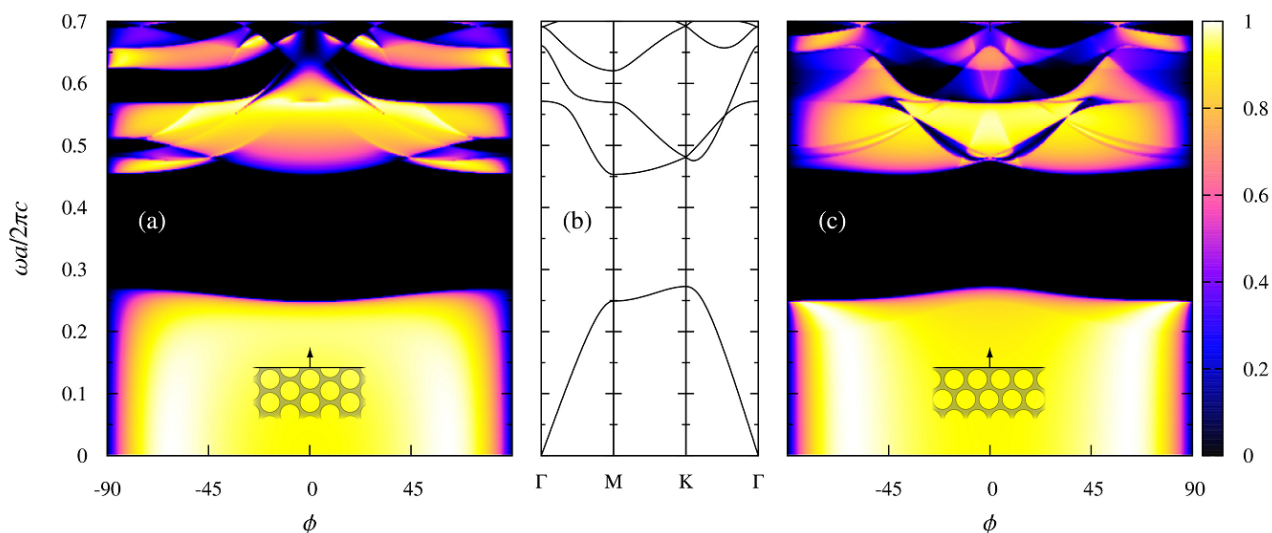
Fig.9: Directional spectral emissivity from a two-dimensional hexagonal lattice of air pores in a silicon dielectric matrix (macroporous silicon Photonic Crystal). The plane of the interface is perpendicular to the Γ-M (panel (a)) or the Γ-K direction (panel (c)). The corresponding photonic bandstructure is depicted in panel (b).

References

- own work with complete titles -

[1]   D. Hermann, M. Schillinger, S.F. Mingaleev, and K. Busch, *Wannier-function based scattering-Matrix-Formalism for Photonic Crystal Circuitry*, J. Opt. Soc. Am. B **25**, 202 (2008)

[2]   D. Hermann, M. Diem, S.F. Mingaleev, A. Garcia-Martin, P. Wölfle, and K. Busch, *Photonic Crystals with Anomalous Dispersion: Unconventional Propagating Modes in the Photonic Band Gap*,. Phys. Rev. B. **77**, 035112 (2008)

[3]   P.W. Nolte, D. Pergande, S.L. Schweizer, M. Geuss, R. Salzer, B.T. Makowski, M. Steinhart, P. Mack, D. Hermann, K. Busch, C. Weder, and R.B. Wehrspohn, *Photonic crystal devices with multiple dyes by consecutive local infiltration of single pores*, Adv. Mater. **22**, 4731 (2010)

[4]   C. Blum, C. Wolff, and K. Busch, *Photonic-Crystal Time-Domain Simulations using Wannier Functions*, Opt. Lett. **36**, 307 (2011)

[5]   K. Busch, C. Blum, A.M. Graham, D. Hermann, M. Köhl, P. Mack, and C. Wolff, *The Photonic Wannier Function Approach to Photonic Crystal Simulations: Status and Perspectives*, J. Mod. Opt. **58**, 365 (2011)

[6]   J. P. Hugonin and P. Lalanne, *Perfectly matched layers as nonlinear coordinate transformations: a generalized formulation*, J. Opt. Soc. Am. B **22**, 1844 (2005)

[7] S. Essig and K. Busch, *Generation of Adaptive Coordinates and their Use in the Fourier Modal Method*, Opt. Express **18**, 23258 (2010)

[8] D. C. Meisel, M. Diem, M. Deubel, F. Perez-Willard, S. Linden, D. Gerthsen, K. Busch, and M. Wegener, *Shrinkage precompensation of holographic three-dimensional photonic-crystal templates*, Adv. Mat. **18**, 2964 (2006)

[9] I. Staude, M. Thiel, S. Essig, C. Wolff, K. Busch, G. von Freymann, and M. Wegener, *Fabrication and characterization of silicon woodpile photonic crystals with a complete bandgap at telecom wavelengths*, Opt. Lett. **35**, 1094 (2010)

[10] I. Staude, G. von Freymann, S. Essig, K. Busch, and M. Wegener, *Waveguides in three-dimensional photonic-band-gap materials by direct laser writing and silicon double inversion*, Opt. Lett. **36**, 67 (2011)

[11] S.G. Romanov, U. Peschel, M. Bardosova, S. Essig, and K. Busch, *Suppression of the critical angle of diffraction in thin-film opal-like photonic crystals*, Phys. Rev. B **82**, 115403 (2010)

[12] M. Florescu, K. Busch, and J. Dowling, *Thermal Radiation in Photonic Crystals*. Phys. Rev. B. **75**, 201101(R) (2007)

[13] C. Schuler, C. Wolff, K. Busch, and M. Florescu, *Thermal Emission from Finite Photonic Crystals*, Appl. Phys. Lett. **95**, 241103 (2009)

[14] K. Busch, S. F. Mingaleev, M. Schillinger, and D. Hermann, *The Wannier Function Approach to Photonic Crystal Circuits*, J. Phys.: Cond. Mat. **15**, R1233 (2003)

[15] N. Marzari and D. Vanderbilt, Phys. Rev. B **56**, 12847 (1997)

[16] I. Souza, N. Marzari, and D. Vanderbilt, Phys. Rev. B **65**, 035109 (2002)

[17] L. Li, J. Opt. Soc. Am. A **14**, 2758 (1997)

[18] D. M. Whittaker and I. S. Culshaw, Phys. Rev. B **60**, 2610 (1999)

[19] T. Weiss, G. Granet, N.A. Gippius, S.G. Tikhodeev, and H. Giessen, Opt. Express **17**, 8051 (2009)

[20] S. F. Mingaleev, A. Miroshnichenko, Y. Kivshar, and K. Busch, *All optical switching, bistability, and slow light transmission in photonic crystal waveguide resonator structures*, Phys. Rev. E **74**, 046603 (2006)

[21] J. G. Fleming, S.-Y. Lin, I. El-Kady, R. Biswas, and K. M. Ho, Nature **417**, 52 (2002); S.-Y. Lin, J. G. Fleming, E. Chow, J. Bur, K. K. Choi, and A. Goldberg, Phys. Rev. B **62**, 2243(R) (2000)

[22] C. S. Kee, S. S. Oh, K. J. Chang, J. E. Kim, H. Y. Park, and K. H. Lee, Phys. Rev. B **60**, 10573 (1999); S.Y. Lin, Phys. Rev. B **66**, 241103(R) (2002)